Minerals Engineering 151 (2020) 106338

Contents lists available at ScienceDirect

Minerals Engineering

journal homepage: www.elsevier.com/locate/mineng

Influence of jaw crusher parameters on the quality of primary crushed aggregates

Marit Fladvad[a,b,*], Tero Onnela[c]

[a] Department of Geoscience and Petroleum, NTNU – Norwegian University of Science and Technology, S.P. Andersens veg 15a, 7031 Trondheim, Norway
[b] Norwegian Public Roads Administration, Abels gate 5, 7030 Trondheim, Norway
[c] Metso Minerals, Lokomonkatu 3, 33100 Tampere, Finland

ARTICLE INFO

Keywords:
Construction aggregates
Jaw crusher
Parameter study
Aggregate quality
Crusher operation

ABSTRACT

A parameter study using a jaw crusher is designed to investigate the influence of feed gradation, feed rate, crusher setting and crusher speed on the crusher operation and the quality of the produced aggregates. The study is focused on the production of all-in large-size (top size ⩾90 mm) aggregates, suitable for use in subbase and frost protection layers in a pavement structure. Aggregate quality is measured in terms of product gradation, particle shape and mechanical properties.

Feed gradation, crusher setting and crusher speed affects the specific energy consumption during crushing. Particle shape is affected by all parameters; feed gradation, feed rate, crusher setting and crusher speed. Mechanical properties are least affected by the jaw crusher parameters, but sample preparation using laboratory crushing clearly affect mechanical properties.

The results from this study provide valuable knowledge for the optimisation of single-stage crushing regarding crusher operation and aggregate quality. By adapting the crushing process to the available feed material and desired product, the quality of the crushed product can be optimised along with the crusher operation.

1. Introduction

In road construction, local aggregate resources can be utilised through aggregate production on the construction site. The aggregate production process, where construction aggregates are produced from bedrock, often involves several crushing steps. The output is normally considered a product after two or more crushing stages. However, primary, or single-stage, crushed aggregate materials can be used as products in road construction, in e.g. unbound subbase and frost protection layers. Such productions usually involve a simple setup with mobile crushing equipment. Research into aggregate production and quality have traditionally been focused on products from subsequent crushing stages, not products from primary crushing. There is a knowledge gap regarding the influence of the crushing process on the quality of primary crushed aggregates.

Compared to many other countries, the Norwegian practice for aggregate use, with particle sizes up towards 300 mm in the pavement structure is uncommon. In a survey, Fladvad et al. (2017) found that 12 of 17 surveyed countries restrict material sizes for unbound aggregates to 100 mm or smaller, including the US, UK, Austria, Denmark and Iceland. This is profoundly different from the Norwegian design guidelines (Norwegian Public Roads Administration, 2018), which specifies the gradings 22/125 mm and 22/180 mm as common subbase materials.

The European standards for aggregates (EN 13242, 2007; EN 13285, 2018) are only valid for materials with an upper sieve size of 90 mm or smaller. This size limitation to the standards introduces challenges for producers and costumers because local specifications for aggregate products must be created. One such local specification is the new Norwegian standard for large-size construction aggregates, which defines common methods for description and quality assessment for large-size aggregates (NS 3468, 2019).

Quality assessment of aggregates is mainly ruled by tests regarding mechanical strength for the rock type in question. These tests are related to the rock deposit, and test results are regarded as representative for all aggregate gradings produced from the source rock. The current requirements for mechanical aggregate properties are based on laboratory testing of crushed material in standardised fractions. When the materials used in the pavement structure are of a coarser size fraction than what is required for the laboratory tests, the material tested has to

* Corresponding author at: Department of Geoscience and Petroleum, NTNU – Norwegian University of Science and Technology, S.P. Andersens veg 15a, 7031 Trondheim, Norway.
E-mail address: marit.fladvad@ntnu.no (M. Fladvad).

https://doi.org/10.1016/j.mineng.2020.106338
Received 19 July 2019; Received in revised form 30 November 2019; Accepted 9 March 2020

be crushed down to the appropriate size in the laboratory. This practice implies the assumption that aggregate properties are predominantly determined by the geological origin of the resource (i.e. mineralogy, petrology), and only negligibly influenced by the production, e.g. blasting and crushing.

A growing focus on the utilisation of local aggregate resources at construction sites has increased the interest in the quality of primary crushed aggregates in Norway. The construction of long tunnels has created a surplus of hard rock resources in several road and railway construction projects. Large volumes of blasted rock are available at tunnel construction sites, and the production of primary crushed aggregates provides an affordable construction material with low CO_2 emissions from transport. Blasted rock is no longer allowed used in the pavement structure without further processing. The production of local aggregates is conducted by mobile crushing and screening equipment, which both due to economical and space restrictions require a simple setup.

The part of aggregate processing investigated in this paper is the crushing, specifically primary crushing using a jaw crusher. Coarse aggregates for unbound use are often produced using a single crushing stage in a jaw crusher, as opposed to concrete or asphalt aggregates, where at least two and often three or four crushing stages are used, employing several crusher types. Most published literature is focused on the use of cone crushers and several types of impact crushers. There is a gap of knowledge regarding the quality of large-size aggregates, especially coarse aggregates produced in a single-stage crushing plant.

To close this knowledge gap, a jaw crusher parameter test is designed based on previous research into crushing and aggregate production, presented in the following:

As a general rule, the strength of rock increases with decreasing mineral grain diameter (Brace, 1961; Brattli, 1992). Although some rock types are considered more suitable for aggregate production than others, mechanical properties for aggregates cannot be inferred directly from rock type. Erichsen et al. (2008) presented an overview of mechanical tests from a Norwegian aggregate database and concluded that the variation in mechanical properties can be as great within specific rock types as between different rock types. Miskovsky et al. (2004) showed that mineral content influence the mechanical properties, but also that micro-cracks influence the same properties, and hence, incautious production can cause considerable deterioration of the rock material.

Räisänen and Mertamo (2004) found that laboratory crushers can provide aggregates with too good shape properties, leading to overestimation of the aggregate quality, and stated that correlation between laboratory and industrial multi-stage crushing plants cannot be made.

Eloranta (1995) investigated the crushing process with emphasis on particle shape (cubicity) of the produced material, and found that the most important properties are the feed gradation and crusher stroke. These findings were based on full-scale tests with gyratory and cone crushers. Based on these tests, Eloranta (1995) presented guidelines for crushing when the goal is to produce cubical aggregates. These guidelines differentiate on whether the feed material contains fines.

Briggs and Evertsson (1998) also focused on product shape, and after testing materials in the size range 16–40 mm, found that the operation of the crusher to a large degree influences aggregate shape. They found that multi-point loading creates better-shaped products than single-point loading, and further that efficient size reduction and improvement of shape are two mutually excluding objectives.

The subject for Bengtsson (2009) was product quality with focus on particle shape, after secondary and tertiary crushing. Among his findings were empirical models showing that crusher setting, feed size, crusher speed and throw affects particle shape in products from cone crushers. Increased average feed size increases flakiness index, likewise does decreased crusher speed. Further, Bengtsson states that in full-scale crushing, there is no evidence that feed shape affects product shape.

Bouquety et al. (2007) investigated the influence of crusher setting and feed grading on the shape of products from tertiary crushing, and found that shape varies within the product gradation with increasing flakiness for decreasing particle size. Consequently, they conclude that increased product size results in better shape.

Johansson et al. (2017) presented a fundamental model of a industrial-scale jaw crusher based on previous studies of cone crushers. The model predicts capacity and power draw for various speeds and crusher settings.

When testing several materials from one deposit, Andersson and Öjerborn (2014) found that the particle shape (flakiness) of a material affects its resistance to fragmentation measured by the Los Angeles abrasion test. Benediktsson (2015) artificially varied the amount of flaky particles in samples for mechanical testing, and found that flakiness affects the results from mechanical testing. In addition to material broken down to 1.6 mm or smaller as described in the test specification, Benediktsson also measured the amount of material left in the original test size after testing. The general trend found was that the mechanical results are improved by reduced flakiness in the sample.

Guimaraes et al. (2007) found that energy consumption during crushing increases with increasing fines generation, because the energy required is proportional to the amount of new surface created.

Lee (2012) researched compressive crushing with a goal of optimising the product yield (amount of valuable product compared to by-products) and energy consumption, with focus on cone crushers. Among her findings was that to optimise product yield, interparticle crushing should be held at a minimum. Particle shape was not considered in Lees studies.

Cook et al. (2017) investigated aggregate mixtures from four different rock types, and found that particle shape affects the packing density of unbound aggregates, especially for open-graded mixes. Further, they found that micro-Deval value is mainly decided by mineralogy, but that particle shape can also affect the value. Increasing flatness led to increasing micro-Deval value. Erichsen et al. (2011) describes differences and similarities between the mechanical tests for aggregates, and highlights their empirical nature. Furthermore, in Erichsen (2015), a new method for presenting the results from the mechanical tests is proposed. Coronado et al. (2011) conducted an experimental study on unbound granular pavement materials, aiming to develop a material ranking based on mechanical behaviour rather than empirical tests such as the Los Angeles and micro-Deval tests. They found that the ranking provided by empirical tests on samples of a set particle size range does not match the performance of the same aggregates when the full gradation is tested in a triaxial test.

None of the presented research had focus on products from primary crushing. For applications where large-size aggregates are used, such as unbound aggregates for road structures, single-stage crushing can be applied. The interest of the current research is to conduct full-scale tests with jaw crushers in the primary crushing stage, to gain knowledge about how a single crushing stage after blasting can affect the quality of the produced aggregate. The aim is to verify whether relations known from research into finer aggregates produced using more than one crushing stage are valid also for large-size aggregates produced from primary crushing. The hypothesis used in the research design is: Crushing efficiency and product quality can be optimised by adjustments to crusher and feed parameters. Crushing efficiency can be measured as capacity and energy consumption. Product quality is measured in terms of particle shape and mechanical properties. The crusher and feed parameters used are closed side setting (*CSS*), speed, feed rate and feed gradation.

This paper presents a parameter study investigating the effect of feed and jaw crusher parameters on the quality of aggregates produced from single-stage crushing. The parameter study is evaluated using mechanical and geometrical tests for aggregate properties. In order to keep the focus on the gradation and crusher parameters, the study is limited to one rock type. The aggregates produced during the study are

in the size range 0–125 mm.

2. Materials and methods

2.1. Test material

To correlate the production parameters with the resulting aggregate properties, the geological properties were held constant while the crusher properties were changed. The test was therefore restricted to a single rock type. The material tested was a granodiorite, a coarse-grained intrusive igneous rock from Nokia, Finland. The test material was supplied from an open-pit quarry in regular operation.

The test material was pre-assessed through testing of its resistance to fragmentation (Los Angeles test, EN 1097-2 (2010)) and resistance to wear (micro-Deval test, EN 1097-1 (2011)), and found to be suitable for unbound use in road construction following Norwegian requirements (Norwegian Public Roads Administration, 2014). The declared values for mechanical strength are given in Table 1.

The blasted rock material supplied to the test plant was in the 0/500 mm[1] size range, the maximum particle size (D_{max}) stretching to 630 mm. The material was produced by drilling and blasting and had not been crushed previously. The blasting was conducted using a borehole diameter of 83 mm, borehole spacing of 3 m, and burden of 2.3 m. In the quarry, a hydraulic hammer had been used to split oversize rocks down to the desired top size. To avoid jamming the crusher, the input material was also assessed visually at the test plant, and oversized particles were removed manually before the material was fed to the crusher.

To create variations in minimum and maximum size of the feed material, the materials were scalped at the test plant before being fed to the jaw crusher. The scalper had elongated openings with slot widths 100 mm and 225 mm. The oversize removal and scalping process enabled the production of five particle size fractions (d/D):

- 0/400 mm
- 100/400 mm
- 180/400 mm
- 0/300 mm
- 100/300 mm

The particle size distributions for the five feed sizes are shown in Fig. 1. Due to the allowance for over- and undersize in the naming of particle size fractions, the sizes d and D are not identical to the scalper slot widths.

Although each test was run in minimum three parallels with identical test portion preparation, there is variation in the sizes for every feed material. To account for these variations, the sizes F_{10} and F_{90} will be used instead of the theoretical d and D in the presentation of individual results. F_{10} and F_{90} are the sizes which 10% and 90% of the feed materials passes, respectively. These sizes are easily recognised from the PSD curves as the sizes at which the curve passes the 10% or 90% lines.

2.2. Methods

2.2.1. Full-scale crushing test

The test setup followed the process flow sheet in Fig. 2. Blue rectangles illustrate processes; green parallelograms illustrate outputs used for further analysis, while yellow ellipses are products not further analysed.

Table 1
Declared values for mechanical properties of test material.

Test method	Test result
Resistance to fragmentation (Los Angeles), EN 1097-2	$LA = 28$
Resistance to wear (micro-Deval), EN 1097-1	$M_{DE} = 9$

The tests were conducted using a Nordberg C80 jaw crusher. The crusher has an opening of 800 x 500 mm; the recommended maximum material size for this crusher is specified to 410 mm. The crusher was fed by a vibrating feeder with adjustable feed rate.

The stroke of the crusher was constant at 30 mm, while three *CSS* were used: 40 mm, 70 mm, and 100 mm. The normal speed for the crusher was 355 rpm. A reduced speed of 284 rpm was also tested, corresponding to a 25% reduction.

Two feed levels were used, defined as high and low feed rate. At the high feed rate, the crusher was choke fed, ensuring the crusher could run at maximum capacity. The low feed rate allowed the crusher to run empty during the crushing; hence involving a lower density of material in the crusher and reduced throughput. The feed rates were not fixed, but manually adjusted by the crusher operator.

A summary of the parameters can be seen in Table 2, while Table 3 shows the full test matrix with the individual parameter combinations. Each of the 12 main tests T4 – T15 in Table 3 was conducted in minimum three parallels.

In each test, a minimum of 1500 kg of blasted rock was crushed. Depending on the feed gradation and the setting of the crusher, the amount of material crushed varied from 1500 kg to 2500 kg.

During testing, the crusher was monitored, and data for power draw was extracted from the monitoring system.

To measure the throughput of the crushing operation, a sample was taken from the output flow from the crusher using a wheel loader during the middle of the test when the crusher was running steadily. This way, the effects of lower quality crushing during starting and stopping of the crushing operation was eliminated from the sampled material. The duration of the sampling was registered, the amount of material was weighed, and from this data, the throughput [tonnes/hour] of the crushing operation was calculated.

2.2.2. Sampling

Photos for image analysis was taken after the material was loaded onto the feeder, before the feeder was started. The feed gradation curves are calculated using the digital image processing (DIP) software Split-Desktop 4.0, based on one photo from each test feed. The images were scaled by two 250 mm spheres included in the image with the feed material. Consistency in the DIP was ensured by analysing a share of the images separately by two different analysts, and the results were compared with compliant results.

Material samples for particle size distribution analysis were taken from each crushing test by extracting material directly from the output conveyor from the crusher using a wheel loader. The amount of material in these samples varied from 130 kg to 430 kg, depending on the expected gradation. To avoid segregation and ensure representativity, the full test portion from the wheel loader bucket was collected.

The remaining material after a finished test was then screened to extract 8–16 mm material for mechanical testing. Samples of minimum 50 kg 8–16 mm were collected from each test product.

2.2.3. Laboratory testing

Particle size distribution.

The particle size distribution for the product from each test was measured combining manual sieving for the material > 90 mm, and mechanical sieving for the material < 90 mm.

Following NS 3468 (2019), the samples were sieved manually with

[1] Throughout this paper, aggregate sizes are described as following the notation from EN 13242 (2007): d/D denotes an aggregate particle size distribution where up to 20% over- and undersize particles are present, while d–D signifies a distribution where all particles are in the size range from d to D, with no under- or oversize. d = lower sieve size; D = upper sieve size.

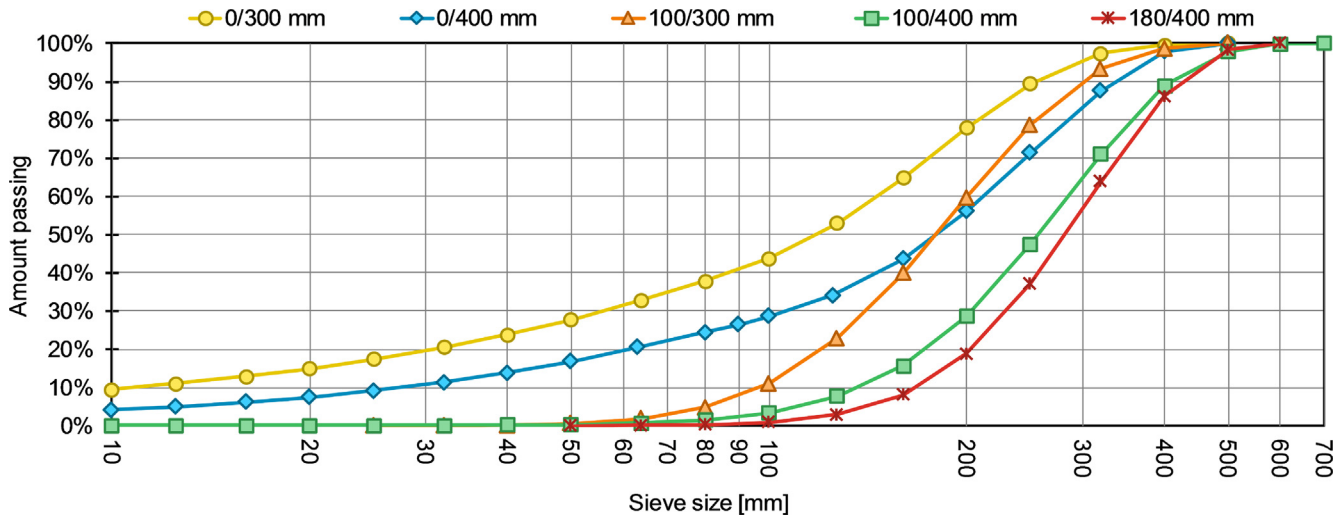

Fig. 1. Feed material particle size distributions from image analysis. Each line represents average values from all tested materials of each size fraction.

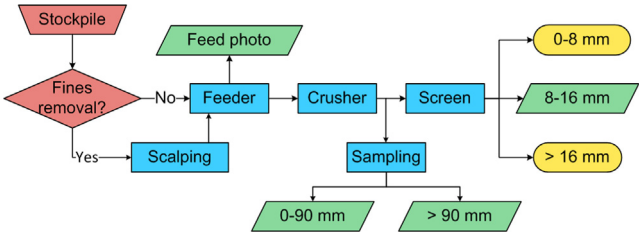

Fig. 2. Process flow sheet for the crushing tests, including sampling for laboratory testing.

Table 2
Summary of available settings of the feed and crusher parameters.

Parameter	Available settings
Lower feed material size (*d*)	0, 100, 180 mm
Upper feed material size (*D*)	300, 400 mm
Feed level	High, low
Closed side setting (*CSS*)	40, 70, 100 mm
Crusher speed	355, 284 rpm

Table 3
Parameter combinations used during testing.

Test ID	Feed material size [mm]	Feed level	Closed side setting [mm]	Crusher speed [rpm]
T4	100/400	High	70	355
T5	100/400	Low	70	355
T6	100/400	High	40	355
T7	100/400	High	100	355
T8	180/400	High	70	355
T9	0/300	High	40	355
T10	0/300	High	70	355
T11	100/300	Low	40	355
T12	100/300	High	40	355
T13	100/300	High	70	355
T14	0/400	High	70	284
T15	100/400	High	70	284

a 90 mm field sieve at the crushing site, and all material smaller than 90 mm was brought to the laboratory for further testing. Material larger than 90 mm was sieved manually at the crushing site with sieves of sizes 100, 125, 160 and 200 mm. This method was chosen in order to reduce the sample sizes brought to the laboratory. After the 90 mm split, the resulting size of the samples brought to the laboratory varied from 90 to 270 kg. In the laboratory, large samples were divided and reduced using a riffle box, always keeping a sample of minimum 80 kg for the PSD analysis.

The mechanical sieving method was based on standard EN 933-1 (EN 933-1, 2012), with the following adjustments:

- Smallest sieve size used: 1 mm
- The test portions were not washed prior to sieving; the analysis followed the procedure for dry sieving
- For some samples, material < 25 mm was subsampled to minimum 6.3 kg using a riffle box before sieving continued

Table 4 contains an overview of the sieves used. The minimum sieve size of 1 mm was chosen because this research is mainly concerned with the coarse part of the particle size distribution curve. By using these sieve sizes, washing and drying of the samples could be avoided. The samples were stored indoors for several months prior to sieving; hence, moisture was not a problem during sieving.

Particle shape. The particle shape of the product material was measured using the flakiness index method (EN 933-3, 2012), which is valid

Table 4
Particle size fractions and related sieve sizes used for the laboratory analyses. Square sieves are used for analysis of particle size distributions, bar sieves are used for analysis of flakiness.

Particle size fraction	Aperture size,square sieve	Slot width,bar sieve
> 200 mm	200.0 mm	125.00 mm
160–200 mm	160.0 mm	100.00 mm
125–160 mm	125.0 mm	80.00 mm
100–125 mm	100.0 mm	63.00 mm
90–100 mm	90.0 mm	50.00 mm
80–90 mm	80.0 mm	40.00 mm
63–80 mm	63.0 mm	40.00 mm
50–63 mm	50.0 mm	31.50 mm
40–50 mm	40.0 mm	25.00 mm
31.5–40 mm	31.5 mm	20.00 mm
25–31.5 mm	25.0 mm	16.00 mm
20–25 mm	20.0 mm	12.50 mm
16–20 mm	16.0 mm	10.00 mm
12.5–16 mm	12.5 mm	8.00 mm
10–12.5 mm	10.0 mm	6.30 mm
8–10 mm	8.0 mm	5.00 mm
6.3–8 mm	6.3 mm	4.00 mm
5–6.3 mm	5.0 mm	3.15 mm
4–5 mm	4.0 mm	2.50 mm
2–4 mm	2.0 mm	–
1–2 mm	1.0 mm	–

for material in the size range 4–100 mm. The samples were analysed using standard laboratory sieves for the 0–90 mm product samples brought to the laboratory. In addition, the material > 90 mm which were sieved manually for size distribution at the test site was also manually sieved for particle shape analysis using custom-made bar sieves with slot widths of 50, 63, 80, 100, and 125 mm. The individual particle fractions used are shown in Table 4, starting with 4–5 mm as the smallest fraction.

$$FI = 100\,\frac{M_2}{M_1} \tag{1}$$

According to the standard, the flakiness index is calculated from Eq. 1, where

M_1 is the sum of the masses of the particles in each of the particle size fractions d_i–D_i in grams

M_2 is the sum of the masses of the particles in each particle size fraction passing the corresponding bar sieve of slot width $0.5D_i$ in grams.

Mechanical properties. Resistance to wear was measured using the micro-Deval test (EN 1097-1, 2011), and resistance to fragmentation was measured using the Los Angeles test (EN 1097-2, 2010). Both tests require 10–14 mm test material. Each test was done twice for each product sample: First, the test portions were prepared by sieving 8–16 mm material from the primary crushing. Next, 63–90 mm material from the primary crushing was laboratory crushed to obtain the 10–14 mm test size. In addition to recording the mass retained on the 1.6 mm sieve after testing as the standards specify, mass retained on the 10 mm sieve was also recorded for both test methods. This was chosen in order to quantify how much of the test portion is left in the original test fraction after testing.

The laboratory crushing followed the method description from Norwegian Public Roads Administration (2016). The sample is crushed twice, using a laboratory jaw crusher with setting 11 mm. In the first crushing stage, 63–90 mm rock particles are crushed individually. In the second crushing stage, the product from the first crushing stage is loaded into the crusher in a single batch. The amount of material used in laboratory crushing is minimum 30 kg. The crusher was tested at several settings, and 11 mm was chosen because this was the setting which generated the most material in the 10–14 mm size range.

3. Results

3.1. Crusher operation

When the crusher is fed at the high feed rate, the measured throughput can be characterised as the capacity of the crushing operation. This capacity varied from 77.8 t/h to 194.3 t/h. The highest capacity is registered for the tests including fines in the feed material. Reducing the feed rate resulted in a 50–56% reduction of the throughput.

The capacity of the crushing operation can be modelled using regression analysis combining categorical and continuous predictors. Regression analysis for capacity using *CSS* and the lower size of the feed material (F_{10}) results in a coefficient of determination $r^2 = 0.77$. The relation is displayed in Fig. 3. The highest capacity is achieved with large *CSS* and low F_{10} size.

Specific energy consumption (*SEC*), consumed energy per tonne of crushed material, is a measure of the efficiency of the crushing process. *SEC* is calculated from the gross power draw and throughput using Eq. 2:

$$SEC = \frac{Power\ draw}{Throughput} \tag{2}$$

The energy demand varied from 0.20 to 0.78 kWh/t. *SEC* can be modelled in a similar way as capacity, accounting for crusher speed in addition to *CSS* and F_{10}. The relation is shown in Fig. 4, with a combined $r^2 = 0.83$.

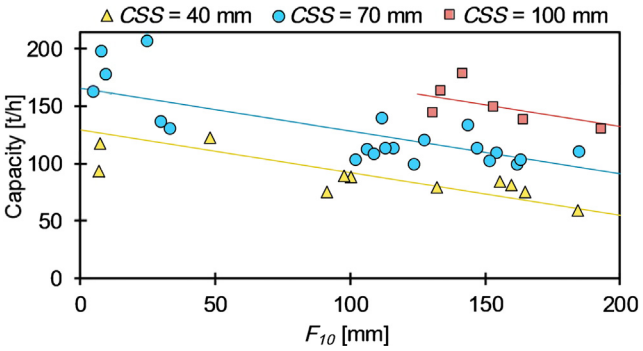

Fig. 3. Capacity vs F_{10}, differentiated by *CSS*. Combined regression analysis: $r^2 = 0.77$.

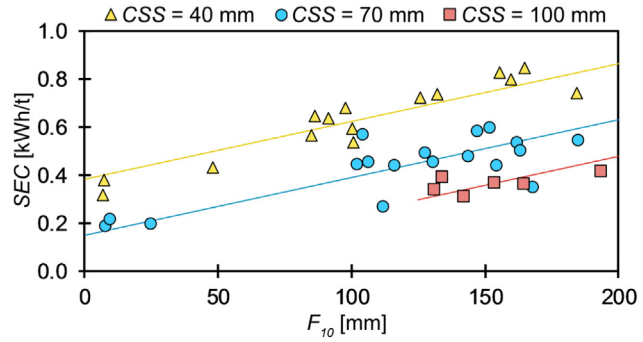

(a) *SEC* vs F_{10}, differentiated by *CSS*

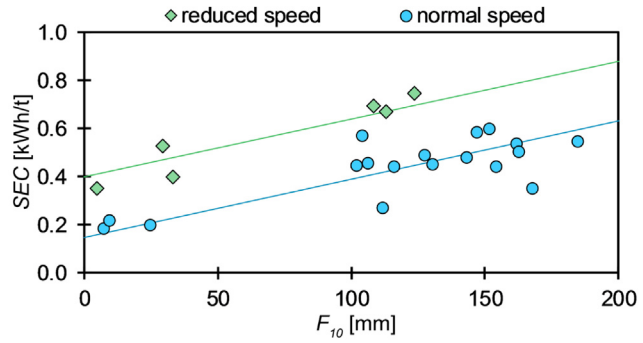

(b) *SEC* vs F_{10}, differentiated by crusher speed

Fig. 4. Specific energy consumption vs F_{10}. Regression analysis combining *SEC*, F_{10}, *CSS* and speed: $r^2 = 0.83$.

Reducing the speed of the crusher results in increased energy consumption per tonne of crushed material. The increase is about 0.25 kWh/t, independent of F_{10}. The lowest energy consumption per tonne is found with high crusher speed, high *CSS* and low F_{10} size.

The test setup did not combine *CSS* = 100 mm with feed materials including fines; hence, the F_{10} range for the *CSS* = 100 line is limited for both capacity (Fig. 3) and *SEC* (Fig. 4a). Reduced crusher speed was only tested for *CSS* = 70 mm; hence, the data points for normal speed in Fig. 4b is also limited to samples where *CSS* = 70 mm.

3.2. Particle size distributions

The effect of changing crusher openings on PSD for feed materials crushed at several *CSS* is shown in Fig. 5. For the tests where the feed did not contain fines, 43–55% of the product material is smaller than

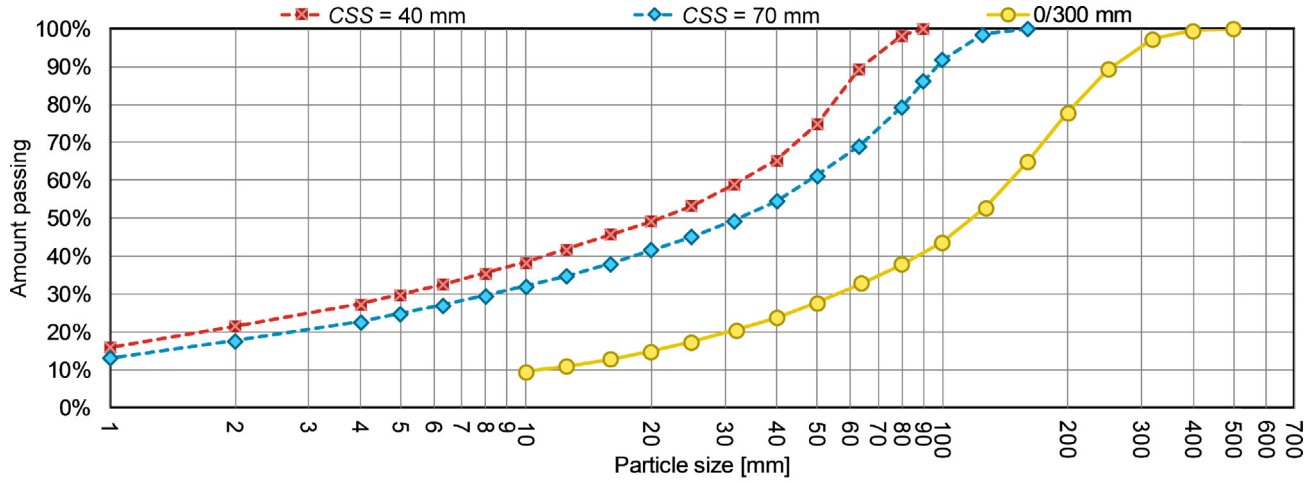

(a) Feed material size 0/300 mm; products from *CSS* 40 and 70 mm.

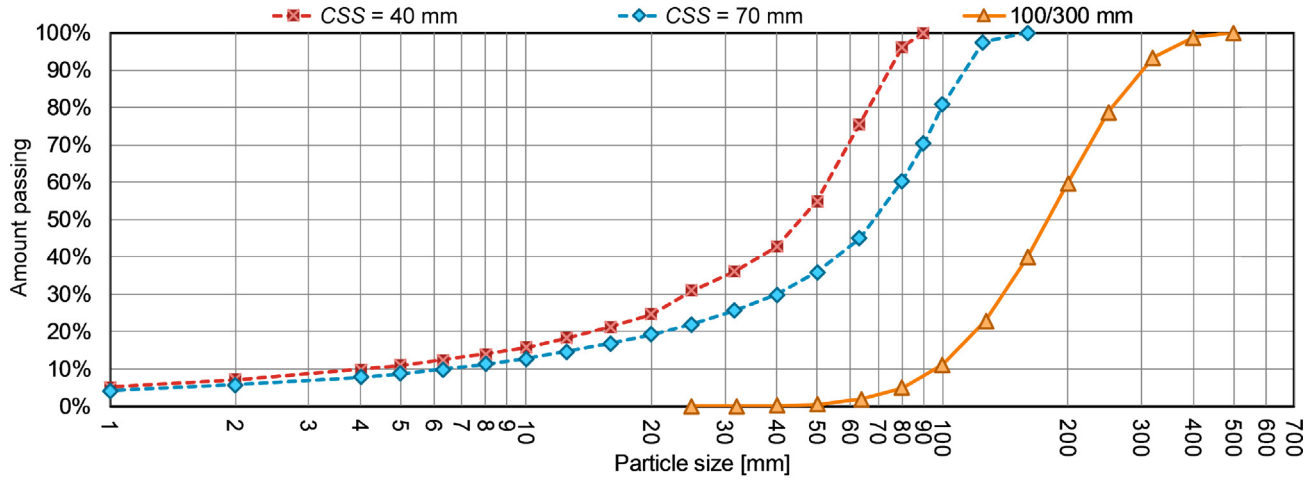

(b) Feed material size 100/300 mm; products from *CSS* 40 and 70 mm

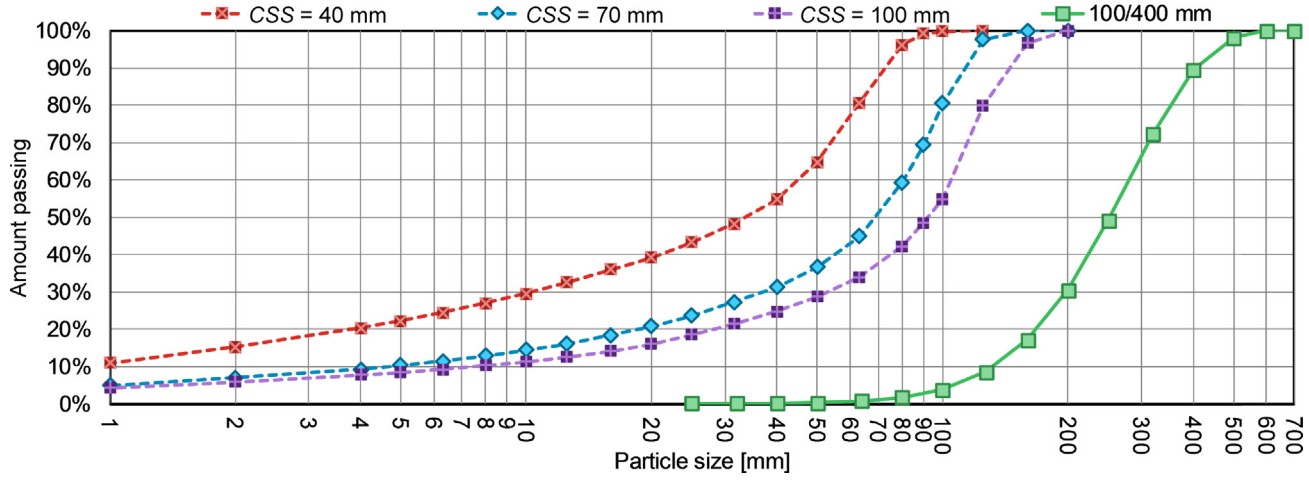

(c) Feed material size 100/400 mm; products from *CSS* 40, 70 and 100 mm

Fig. 5. Particle size distributions for feed and product materials for feed sizes 0/300 mm, 100/300 mm and 100/400 mm. Feed material distributions drawn in solid lines, product distributions in dashed lines. Each line represents the average of minimum 3 parallel tests.

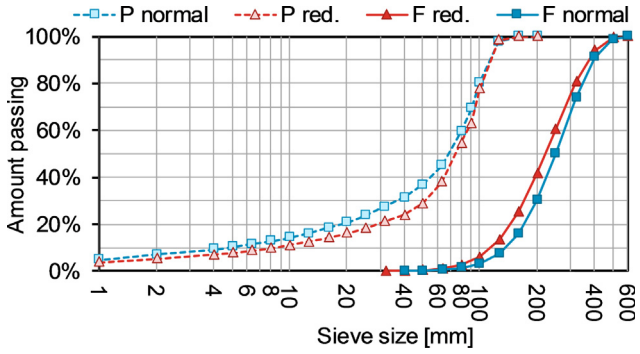

Fig. 6. Feed (F) and product (P) particle size distribution curves for 100/400 mm samples tested at normal and reduced speed. Each line represents the average of minimum 3 parallel tests.

CSS. For the feed material containing fines, the increase in material smaller than *CSS* in the product is about 40 percentage points. More than 96% of the product is smaller than 2·*CSS*, except for T11 where 92% is smaller than 2·*CSS*.

The effect of reduced crusher speed on PSD is seen in Fig. 6. When the crusher speed is reduced, the endpoints of the PSD curve – the top size and the amount of material smaller than 1 mm – is not affected. On the other hand, the PSD curve is steeper, and there is less material smaller than *CSS*. Although the feed material for the reduced speed test had a somewhat finer distribution with approximately 10 percentage points more material passing 160 mm compared to the feed material for the normal speed test, the product curves have the inverse relationship, where the product from the reduced speed test is coarser. 0/400 mm feed was only tested at the reduced speed, so no comparisons to normal speed can be made for this feed material.

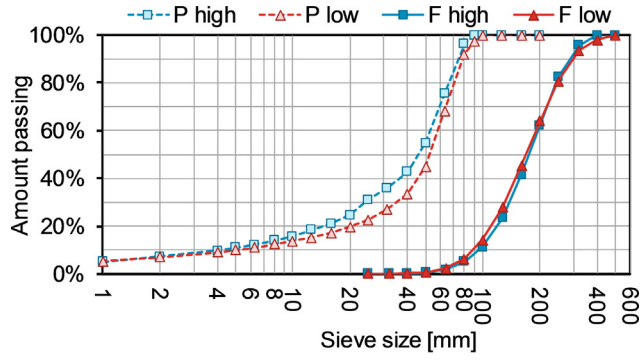

(a) Feed size 100/300 mm

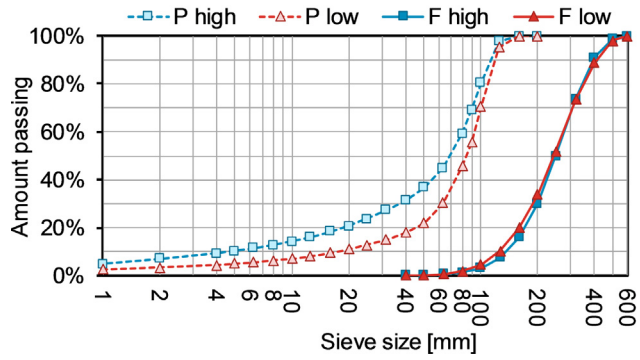

(b) Feed size 100/400 mm

Fig. 7. Feed (F) and product (P) particle size distribution curves for samples tested at high and low feed rate. Each line represents the average of minimum 3 parallel tests.

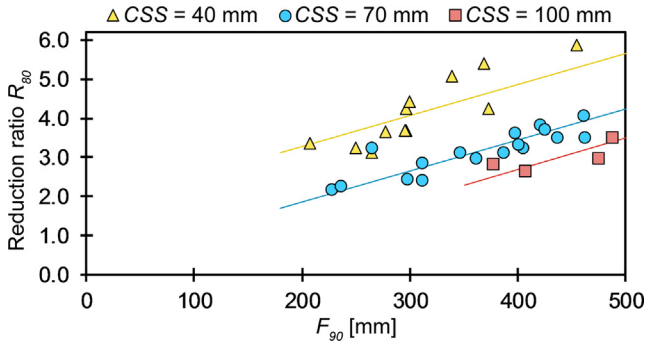

Fig. 8. Reduction ratio R_{80} vs. the upper size for the feed material F_{90}, differentiated by closed side setting *CSS*. Regression analysis combining R_{80}, F_{90} and *CSS*: $r^2 = 0.808$.

The effect of reduced feed rate on the PSD is seen in Fig. 7. The reduced feed rate results in a 25% reduction in the amount of material smaller than *CSS*. The reduction is significant at the 99% confidence level. Reducing the feed rate does not affect the top size of the product.

3.3. Reduction ratio

The reduction ratio for each test is calculated as the ratio between the respective screen sizes through which 80% of the feed and product distribution passes (Eq. 3):

$$R_{80} = \frac{F_{80}}{P_{80}} \tag{3}$$

The test setup resulted in a span of reduction ratios for each *CSS*, as seen in Fig. 8. Among all tests, R_{80} ranged from a minimum of 2.2 to a maximum of 5.9.

R_{80} can be reliably predicted from the ratio between F_{90} and *CSS* using Eq. 4 with $r^2 = 0.842$. The relation is shown in Fig. 9, with the symbols from Fig. 8 kept for comparison.

$$R_{80} = 0.997 + 0.4155\frac{F_{90}}{CSS} \tag{4}$$

When the speed of the crusher was reduced by 25% from 355 to 284 rpm, R_{80} was reduced by about 0.5. This difference is statistically significant at the 95% confidence level.

The samples crushed at reduced feed rate had a somewhat reduced R_{80}, but the difference is too small to be statistically significant with the low number of samples (6 tests for reduced feed rate).

3.4. Particle shape

As seen in Section 3.2, the top size of the product from each test is related to *CSS* ($P_{96} \approx 2$CSS). To enable comparison of the particle shape

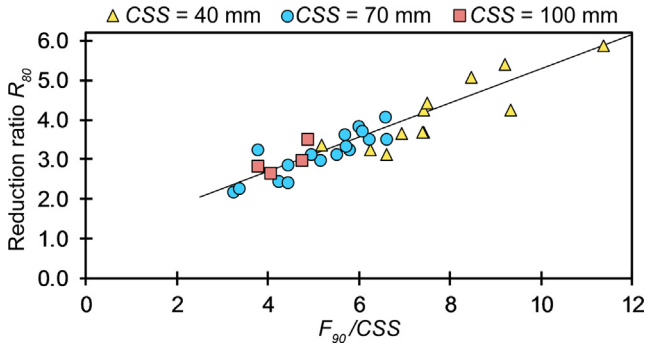

Fig. 9. Reduction ratio R_{80} as a function of the ratio between the upper size for the feed material F_{90} and the crusher setting *CSS*; $r^2 = 0.842$.

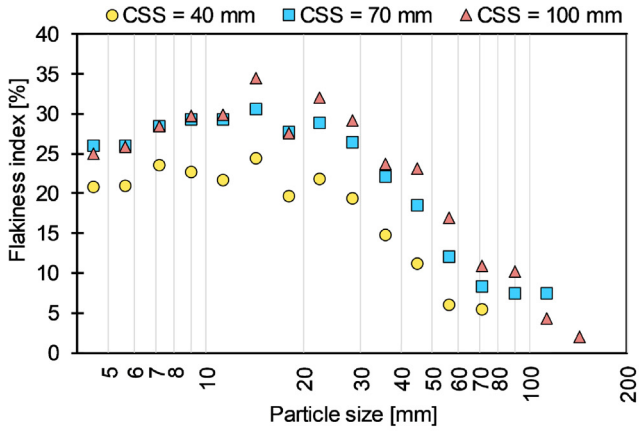

(a) *FI* compared at different *CSS*

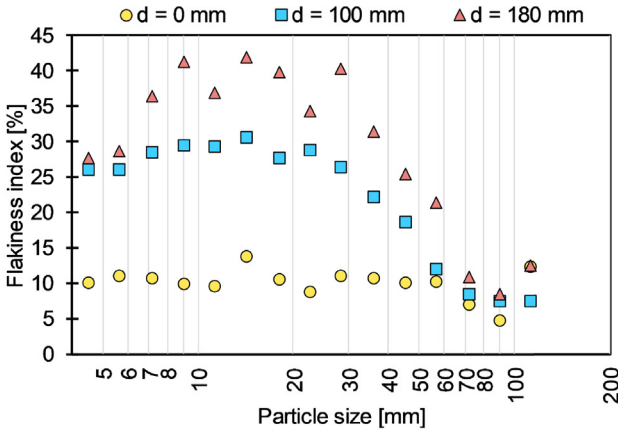

(b) *FI* compared at different lower feed size *d*

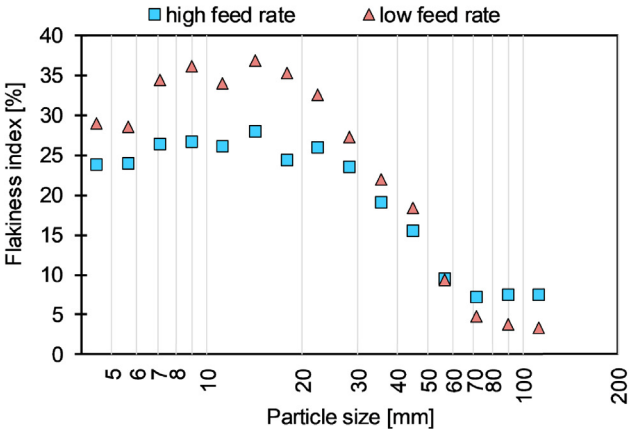

(c) *FI* compared at high and low feed rate

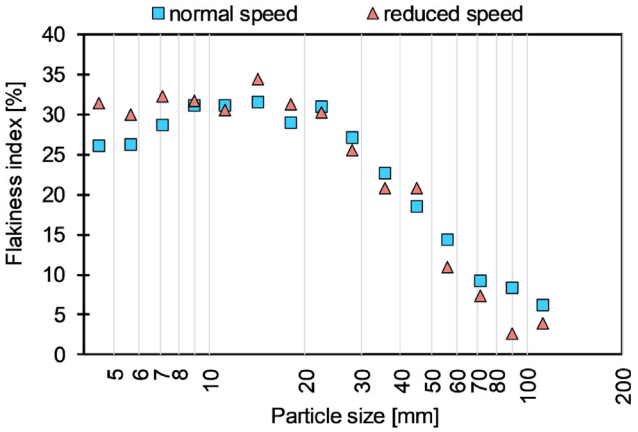

(d) *FI* compared at normal and reduced crusher speed

Fig. 10. Particle shape measured as flakiness index for individual particle size fractions. The x-axis displays the middle size of each particle size fraction.

for the full product gradations, the results will be presented for the size range 4 mm–2*CSS* ($FI_{<2CSS}$), rather than the standard calculation for 4–100 mm (FI_{4-100}).

The average $FI_{<2CSS}$ for all tests is 11.8, but the *FI* of the product is considerably different for material above and below *CSS*. $FI_{<CSS}$ varies from 8 to 33 with an average value of 20.3, while $FI_{>CSS}$ varies between 0 and 15 with an average value of 6.7. Products above *CSS* are less flaky and there is less variation in particle shape than below *CSS*.

The general trend for *FI* vs particle size can be seen in Fig. 10a; *FI* is lower for larger particles, and increases with decreasing particle size until a maximum is reached for the 12.5–16 mm size fraction. Below this size, the *FI* is stable (*CSS* = 40 mm) or somewhat decreasing (*CSS* = 70 and 100 mm). The maximum *FI* is found at the same particle size independent of *CSS*.

Another general tendency in Fig. 10a is that for a specific size fraction, *FI* is lower for products produced at lower *CSS*. In contrast, $FI_{<2CSS}$ is not affected by*CSS* changing between 40, 70 and 100 mm, as the value is 12.7 with a variation of only ± 0.3 between the three settings. The results for *FI* vs *CSS* are however somewhat ambiguous, as the difference between *CSS* 40 mm and *CSS* 70 mm in Fig. 10a is clear for all particle sizes, while the difference between FI for *CSS* 70 mm and *CSS* 100 mm for the smaller sizes is minimal.

Including fines in the feed material results in a decreased flakiness index for the product, as seen in Fig. 10b. This effect is consistent for all product sizes from 4–5 mm to 80–100 mm. For the tests where fines were included in the feed, there are only minor differences in *FI* for different particle sizes. *FI* varies between 4.8 and 13.8 for $d = 0$, while the variation is much greater for $d = 100$ (7.5–30.6) and $d = 180$ mm (8.4–41.8).

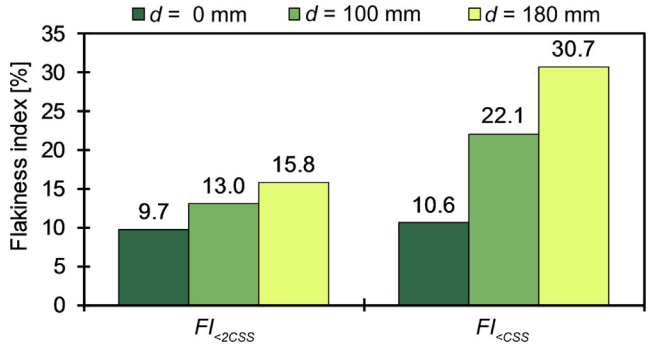

Fig. 11. Global FI ($FI_{<2CSS}$) and FI for product smaller than CSS ($FI_{<CSS}$) depending on lower feed size *d*.

Fig. 11, where $FI_{<2CSS}$ and $FI_{<CSS}$ is compared, shows that the increase is most evident for $FI_{<CSS}$, which doubles when *d* is increased from 0 to 100 mm, and almost triples when *d* is increased from 0 to 180 mm.

The data show good correlation between $FI_{<CSS}$ and F_{10} when feed rate is accounted for ($r^2 = 0.713$), as seen in Fig. 12a; $FI_{<CSS}$ is reduced when smaller material is present in the feed. Although the relationship is weaker than for F_{10}, $FI_{<CSS}$ is also increasing when the F_{90} size increases, showing the general trend that a coarser feed material results in a more flaky product.

Equal correlation is also found between $FI_{<CSS}$ and the amount of

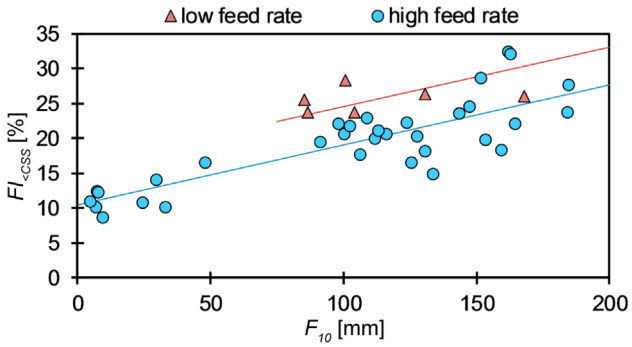

(a) $FI_{<CSS}$ vs F_{10}, differentiated by feed rate. Regression analysis combining $FI_{<CSS}$, F_{10} and feed rate: $r^2 = 0.713$

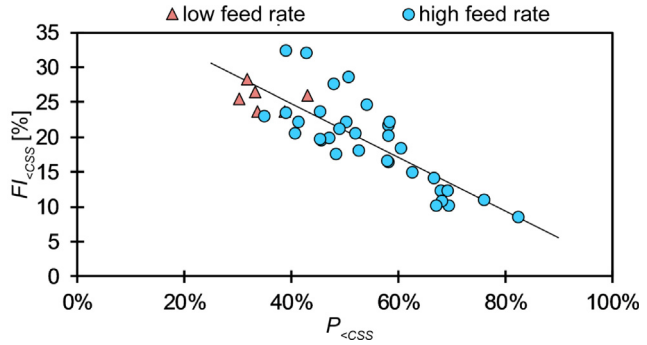

(b) $FI_{<CSS}$ vs amount of product smaller than CSS ($P_{<CSS}$), $r^2 = 0.680$

Fig. 12. *FI* for product smaller than *CSS* ($FI_{<CSS}$) related to feed or product gradation.

material smaller than *CSS* in the product gradation ($r^2 = 0.680$) in Fig. 12b; increased amount of material smaller than *CSS* in the product gives a reduced $FI_{<CSS}$. In this plot, the low feed rate samples fit to the same regression line as the high feed rate samples. The coarser product gradation resulting from the reduced feed rate found Fig. 7 is also visible in Fig. 12b.

Although few samples represent the low feed rate, a trend of increased *FI* for reduced feed rate is seen in Fig. 12a. When the feed rate is lowered, $FI_{<2CSS}$ decreases by 13% from 12.8 to 11.1. $FI_{<CSS}$, on the other hand, increases by 20% from 21.3 to 25.6. The explanation for this is found in Fig. 10c, which shows that when the feed rate is low, FI increases for particles smaller than 50 mm and decreases for particles larger than 63 mm. The increase in *FI* is between 16 and 45% for all individual size fractions below 50 mm.

When the crusher speed is reduced, $FI_{<2CSS}$ decreases by 32% from 13.4 to 9.1, while $FI_{<CSS}$ remains almost unchanged with 23.5 for normal speed and 22.1 for reduced speed. *FI* results for all particle sizes are displayed in Fig. 10d. The results are not consistent, but there are indications of a shift of particle shape distribution when speed is reduced; *FI*is reduced for large particles and increased for small particles.

No correlation is found between R_{80} and flakiness, neither for$FI_{<2CSS}$, $FI_{<CSS}$ or any of the individual size ranges.

3.5. Mechanical tests

Overall average results from mechanical testing of primary crushed material and laboratory crushed material are displayed in Fig. 13. The tests on primary crushed material have an average *LA* of 27.9, while the laboratory crushed material had an average value of 20.7, corresponding to a 26% reduction. M_{DE} is reduced from on average 9.1 for primary crushed to 7.4 for laboratory crushed material, a reduction by 19%. These results are calculated from 38 individual tests for each property, and variations in the measurements are shown by error bars for maximum and minimum in Fig. 13.

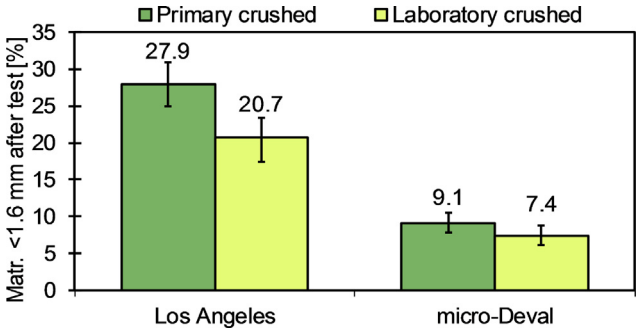

Fig. 13. Mechanical properties measured before and after laboratory crushing (average values). The error bars indicate maximum and minimum values for each data set (N = 38 for each column).

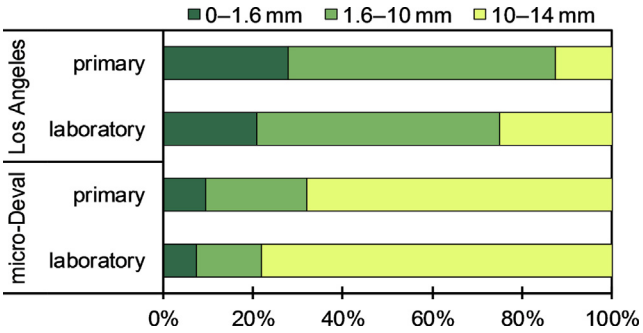

Fig. 14. Size distribution of material after testing by Los Angeles (N = 29) and micro-Deval (N = 25) methods for primary crushed material and laboratory crushed material.

Fig. 14 shows the resulting size distribution for the test portion after the Los Angeles and micro-Deval methods, and how the distribution differs for primary crushed and laboratory crushed samples. The 0–1.6 mm bars represent the standard *LA* and M_{DE} values, while the 10–14 mm bars represent the LA_X and $M_{DE\ X}$ values. As sample preparation by laboratory crushing causes the *LA* value to decreases by 7 percentage points, LA_X increases by 12 percentage points. This shows that the impact of laboratory crushing is largest in terms of the amount of material remaining in the original test size 10–14 mm. This tendency is even clearer for micro-Deval, where laboratory crushing improves M_{DE} from 9.3 to 7.5, while $M_{DE\ X}$ is increased from 68 to 78.

No correlation is found between results for laboratory crushed vs primary crushed material neither for *LA* nor M_{DE}, as Fig. 16 illustrates. The improvement caused by laboratory crushing has shown to be consistent, as all points are gathered on or below the y = x line.

The two measures for mechanical properties are compared in Fig. 15. There is no correlation between Los Angeles abrasion and

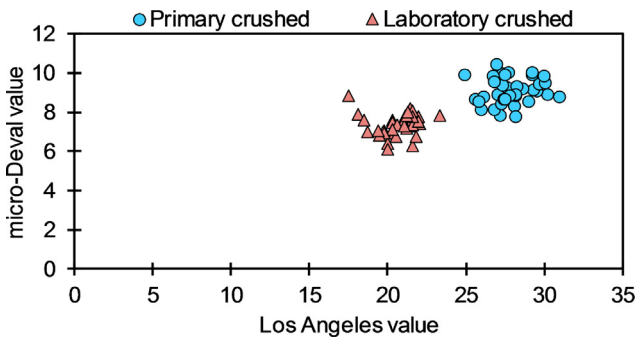

Fig. 15. Micro-Deval vs. Los Angeles test results, for primary and laboratory crushed material.

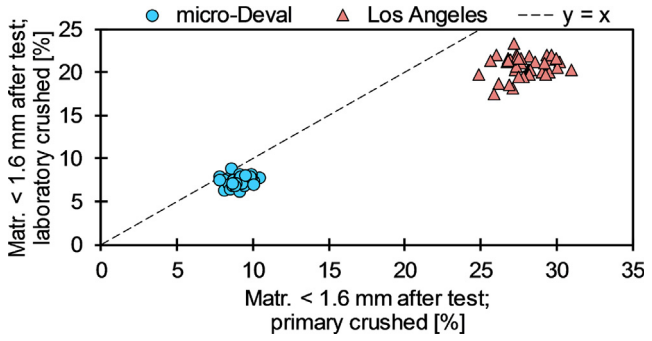

Fig. 16. Test results for laboratory crushed materials vs. primary crushed materials, for micro-Deval and Los Angeles tests.

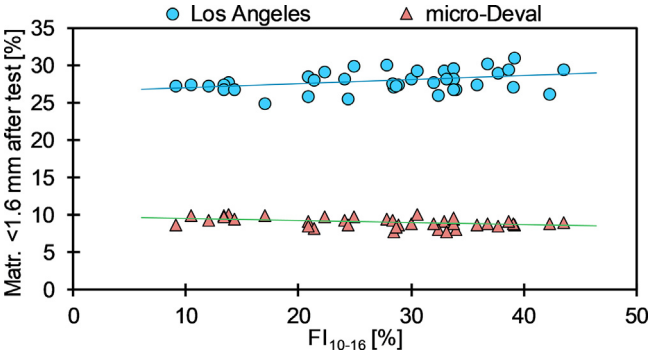

Fig. 17. Mechanical properties vs. flakiness index for particles in the size range used in mechanical testing (10–14 mm). Los Angeles: $r^2 = 0.127$, micro-Deval: $r^2 = 0.188$.

micro-Deval wear, neither for primary crushed nor laboratory crushed aggregates.

In the size range used for mechanical testing (10–16 mm), the test setup provoked variations in *FI* from 9.1 to 43.5. The mechanical properties for the primary crushed aggregates are compared to *FI* for 10–16 mm particles in Fig. 17. Even though the span in *FI* is large, there is no correlation to variation in either *LA* or M_{DE}.

The standard *LA* value does not correlate with any of the other parameters in the dataset. However, the amount of material left in the original test fraction after the *LA* test, LA_X, gives indications of relation both to the amount of product material smaller than *CSS* (Fig. 18a, $r^2 = 0.539$) and the flakiness index for material smaller than *CSS* (Fig. 18b, $r^2 = 0.475$). LA_X increases when the amount of product smaller than *CSS* increases. On the other hand, LA_X decreases when $FI_{<CSS}$ increases.

The closest predictor of M_{DE} found is F_{10}, which can explain 47% of the variation in M_{DE}. Although the variation in M_{DE} is small, the relation between M_{DE} and F_{10} is statistically significant at the 99% confidence level. For higher F_{10} sizes, the measured M_{DE} value is reduced, as seen in Fig. 19.

4. Discussion

4.1. Test material

The average *LA* of granodiorite from Norwegian quarries is about 30, with variation from 17 to 48 for 19 surveyed deposits (Erichsen et al., 2008). The Finnish granodiorite used in the present research had a declared *LA* of 28; thus, the chosen test material is well within the normal quality range for this rock type.

The scalping process successfully enabled the separation of five different feed gradations from the original material provided from the quarry, as seen in Fig. 1. The variation between $d = 0$ and $d = 100$ mm

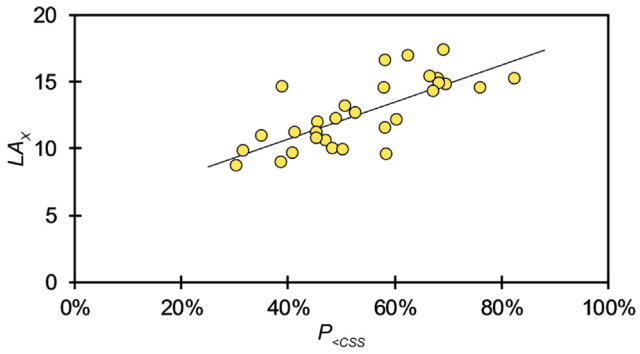

(a) LA_X vs amount of product smaller than *CSS* ($P_{<CSS}$); $r^2 = 0.539$

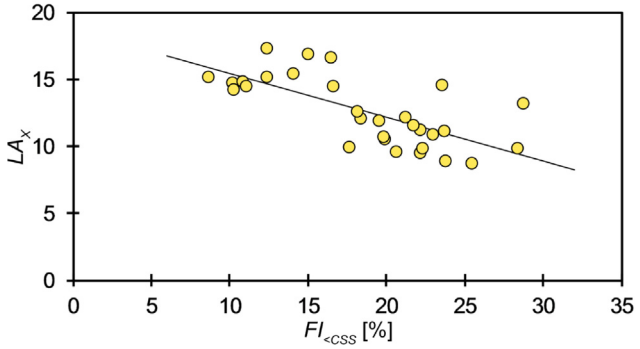

(b) LA_X vs $FI_{<CSS}$; $r^2 = 0.496$

Fig. 18. Possible correlating factors for amount of material left in original test size after LA test (LA_X).

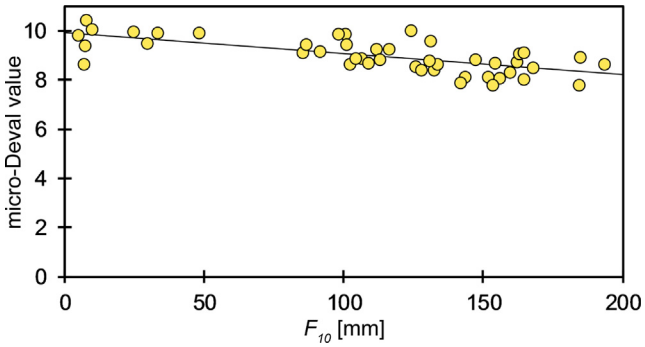

Fig. 19. Micro-Deval value M_{DE} depending on F_{10}; $r^2 = 0.468$.

is used to analyse the effect of keeping fines present in the feed, while $d = 180$ mm can illustrate the effect of segregation in the feed flow, resulting in periods of more uniformly graded feed material.

Due to the lack of suitable laboratory equipment for sieving of large-size materials, PSD for the feed materials are found using digital image processing (DIP). There are few specifications available regarding capturing of images for DIP for full gradation aggregate samples. A standard focused on large-sized aggregates (NS 3468, 2019), published after the tests presented in this paper were conducted, requires a minimum of 400 particles for each analysis. Especially for the coarse samples (e.g. 180–400 mm feed), the conditions are not optimal for DIP due to the limited number of particles visible in each image. For the feed samples containing fines, the number of particles was not a problem.

To obtain valid PSD results for the feed materials from sieving, the whole test portion of 1500–2500 kg should be analysed due to the large particle sizes. The reliability of the results would have improved had the feed samples been sieved, but due to the large particle sizes and

sample weights, this was not feasible. The method of taking photos of the feed material when it was loaded onto the feeder limited the number of particles in the analysis. On the other hand, this method ensured that the particles analysed in DIP were the exact same particles present in each crushing test. Capturing images from the stockpile would enable more particles to be present in each image, but would involve a risk of not uncovering differences in gradation between parallel tests due to segregation. In a production setup with continuous feeding, images could be provided from a conveyor belt feeding the crusher, allowing for the combined analysis of several images to obtain a valid number of particles.

DIP using images from the feeder enabled individual analyses of each feed sample, and the PSD curves in Fig. 1 show that the method was sufficiently accurate to display clear differences between the five chosen feed gradations.

4.2. Setting/reduction ratio

As would be expected, a higher *CSS* increases the capacity of the crushing operation, because a larger opening of the crusher requires less size reduction before the material can be released from the crusher. However, when capacity is differentiated by *CSS* as in Fig. 3, a clear relation is also found between capacity and F_{10}. When smaller particle sizes are present in the feed, more voids between larger particles are filled with smaller particles - the material density in the crusher is increased - and the degree of interparticle crushing increases. At the same time, smaller particles require fewer crushing events before their size is reduced enough to be released from the crusher. Increased density and less required size reduction both contribute to the increase in capacity when the F_{10} size decreases.

Although Fig. 10a shows a considerable reduction in flakiness for a specific particle size when *CSS* is decreased, the overall $FI_{<2CSS}$ and $FI_{<CSS}$ is nearly constant. Hence, the effect of *CSS* depends on the intended screening and use of the products; if the overall particle shape of the full product gradation is of interest, *CSS* can be increased to achieve a coarser product with less *SEC* and higher capacity while maintaining the same global *FI*. However, if the desired quality is related to the material below a certain particle size, reducing *CSS* will result in a more cubical shape of the product at the cost of increased *SEC* and reduced capacity. These results are consistent with the conclusions from Bouquety et al. (2007), who also found that crusher setting influences *FI*of individual size fractions, but not the global *FI*.

Briggs and Evertsson (1998) concluded that efficient size reduction and shape improvement are not possible at the same time, which could imply a positive correlation between the flakiness index and reduction ratio. However, in the current data, no correlation was found between the reduction ratio and particle shape.

4.3. Reduced feed rate

The reduced feed rate corresponded to operating the crusher with a throughput of about half of the capacity. The tests where the feed rate was lowered had the lowest power draw, but the production is inefficient due to the low throughput. The power draw measured for these tests will be affected by the material flow through the crusher not being constant.

The top size of the product was not affected by the feed rate, but the PSD curve is steeper when the feed rate is reduced. The results are ambiguous for fines/lower size because the amount of fines was reduced for the 100/400 mm feed material when feed rate was reduced, while it remained unchanged for the 100/300 mm feed material. The PSD curves show that there is more material in the sizes above *CSS* when the feed rate is reduced.

As the throughput is reduced by about 50%, the reduced material density in the crusher results in less particle-to-particle crushing; hence, the material passing through the crusher will be subject to fewer crushing events. Reducing the feed rate results in a more flaky product for all particle sizes below 50 mm. The increase is largest for material smaller than 25 mm. Yet for the most coarse particles (50–125 mm), *FI* is instead reduced when the feed rate is lowered. Eloranta (1995) stated that choke feeding is necessary to obtain good particle shape. The current results indicate that the trend is the same for a single-stage crushing process using a jaw crusher; the shape is improved at the high feed rate.

The reduced feed rate was tested with feed materials where $d = 100$ mm and *CSS* at 40 mm for 100/300 mm feed and 70 mm for 100/400 mm feed. Thus, there was no material smaller than *CSS* present in the feed in these tests.

4.4. Reduced crusher speed

Reducing the crusher speed results in an increased *SEC* (Fig. 4b), while the PSD curve is steeper (Fig. 6). The particle shape is shifted (Fig. 10d) similarly as described by Bengtsson (2009); smaller particles have higher flakiness. *SEC* is increased as a result of both a reduced throughput and an increased power draw. Guimaraes et al. (2007) found that energy consumption increased when the amount of fines produced increased, but in the current data, the amount of finer material is not increased when energy consumption increases. The results indicate that some of the additional energy consumed when crusher speed is reduced can go towards particle shape improvement for the larger particles, not additional size reduction. These results are, however, limited in that the smallest particle size measured in the current dataset is 1 mm. There could be variations in fines content below this size, which would not be detected by the chosen analysis.

Eloranta (1995) found that increased crusher speed would improve particle shape, i.e. decrease flakiness index. Both Bengtsson and Eloranta note that although altering crusher speed has some effect on the particle shape, the changes become small compared to the impact of other parameters. This is true also for the current dataset; particle shape is more affected by changes in feed gradation, crusher setting or feed rate than crusher speed.

4.5. Flakiness index

For the tests where fines are present in the feed, some of the material assessed after crushing will have passed through the crusher without any size reduction. The improved particle shape when fines are present in the feed could raise the question of whether the feed material had lower *FI* than the crushed material. As no shape characterisation of the material was conducted prior to crushing, this question can not be examined using the present data. However, Bengtsson (2009) did find that feed shape did not affect product shape.

The flakiness index is found to be higher for the smaller particles of a distribution, corresponding to the results from Bouquety et al. (2007). Bengtsson and Evertsson (2006) found that the size range close to the crusher setting had the best particle shape, identified by an increasing FI above CSS. In the current dataset (Fig. 10a), no increase is seen for the largest particles. On the other hand, 12.5–16 mm is identified as the size range where the particles are most flaky.

A deviation from the FI standard is that also larger particles than described in the standard procedure ($>$ 100 mm) was measured in the present data. The calculation of the flakiness index is a weighted average of all individual fractions; thus, the comparison between different materials are affected by their top size. Bouquety et al. (2007) note that differences in flakiness in smaller fractions are hidden by the weighting in the calculation of the global *FI*. Due to the nature of the particle size distribution and the set division into size fractions, the weight of the smallest fractions are considerably smaller than the weight of the largest fractions. For the samples tested in the current dataset, the median weight for the 4–5 mm fraction was 2138 g, while the median weight for the 80–100 mm fraction was 34,926 g.

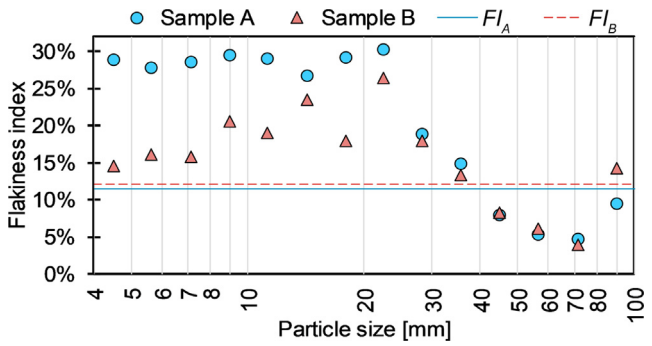

Fig. 20. Comparison of individual fraction *FI* (points) for two test materials of similar $FI_{4–100}$ (lines).

The example in Fig. 20 illustrates the dominating effect of the larger fractions. In this example, sample A has a *FI* higher than or equal to sample B in all fractions except the one analysed using the 50 mm bar sieve. Still, due to the mass of the coarsest fractions, the result is that the standard $FI_{4–100}$ is very similar. *FI* is lower for sample A (11.5) than sample B (12.1) even though the difference in particle shape for the smaller individual fractions is considerable, where sample A have the highest*FI* values. It is clear that the weighted average calculation hides differences in the smaller particle sizes.

In further research on this topic, alternative methods for calculation of *FI* for wide gradations should be investigated. The current standard calculation is reliable for narrow size fractions, but for gradations including the full size range from 4 to 100 mm, differences in particle shape can be hidden. Particle shape is the property most visibly affected when crushing parameters are changed. To investigate the effect of such changes, it is necessary to analyse individual size fractions and not only the weighted average for all sizes.

4.6. Mechanical tests

4.6.1. Preparation of samples

22/125 mm is a common gradation for subbase materials in Norway. The general practice for mechanical testing of such large-size aggregates is to collect a 30 kg sample of the available aggregate (e.g. hand specimens) and prepare the 10–14 mm test portion by laboratory crushing as described in Section 2.2.3. From the results found in Fig. 13, it is apparent that the practice of sample preparation by laboratory crushing affects the reported results. These results match the conclusions from Räisänen and Mertamo (2004) who also found that laboratory crushing resulted in shape properties which were not representative of full-scale crushing conditions.

The lack of relationship between *LA* results for primary and laboratory crushed aggregates in Fig. 15 shows that the laboratory crushing not only improves the test results, but also does not preserve the ranking between stronger and weaker samples. As this experiment is limited to one rock type only, the span of qualities measured is limited with $LA_{primary}$ varying from 24.2 to 31.0.

The general assumption that the results from mechanical tests are an expression for geological properties of the material is refuted, as it is clear that production methods affect the mechanical properties of the material. Thus, mechanical strength should not be assumed constant for all products produced from a specific rock deposit. It is generally accepted that the mechanical properties of an aggregate are improved from each crushing stage because weak minerals are worn off. Hence, there is a risk of overrating the quality of an aggregate when the tested samples are laboratory crushed twice after primary crushing. A sample processed in such a way should not be considered representative for the quality of primary crushed aggregates. When the difference in test result due to sample preparation is as big as 26%, there is a clear risk of ranking alternative available materials wrongfully if the sample preparation is not identical for all samples.

4.6.2. Relation to particle shape

Both Andersson and Öjerborn (2014),Benediktsson (2015) and Cook et al. (2017) found mechanical properties to be related to flakiness. In the current dataset, both *LA* and M_{DE} show poor correlation to *FI* (Fig. 17). Benediktsson (2015) found that the relationship is stronger when *FI* is compared to the remaining material in the original test portion size. For the current data, this is true for LA_X, while there is no improvement in the correlation between $M_{DE\ X}$ and *FI*. Our data show that a decreasing *FI*for the test portion results in more material left in the original test portion size (> 10 mm). Likewise, when the amount of product material smaller than *CSS* increases, more material is left in the original test fraction after the LA test. However, these relations can not explain more than about 50% of the variation in *LA*, so clearly, other factors influence the degradation in the LA test besides particle shape. Particle shape and product gradation are highly correlated, as seen in Fig. 12b, so these factors should not be combined in the prediction of LA_X.

In the current dataset, the largest amount of flaky particles was found in the size range used for mechanical testing. The samples used for laboratory crushing was in the 63–90 mm size range and had a considerably lower *FI*. Furthermore, the two-stage laboratory crushing process is also designed to provide well-shaped products. Based on the presented literature, the difference in particle shape can contribute to the large difference in mechanical properties for primary crushed and laboratory crushed aggregates (Fig. 13).

4.6.3. Relation to gradation

M_{DE} is related to the gradation of the feed material through F_{10} (Fig. 19). Increasing F_{10} leads to a decrease in M_{DE}; i.e. coarser material in the feed results in higher resistance to abrasion. A possible explanation is that fine material can pass through the crusher with low or no size reduction, leading to a high amount of uncrushed particles in the M_{DE} test portion. When the F_{10} size is high, the material tested for M_{DE} has been subject to a bigger size reduction. Although the span of F_{10} is large, the variation in M_{DE} is very small, so the increase in abrasion for smaller feed sizes will not likely have any practical consequences.

There is no correlation between Los Angeles abrasion and micro-Deval wear, neither for primary crushed nor laboratory crushed aggregates. The differences in gradation of the test portions after testing, as seen in Fig. 14, show that different degradation mechanisms are applied and that the two tests are quantifying separate properties. Important differences between the tests are that water is present in the micro-Deval test, and the detrimental forces are higher in the LA test. The findings from Fladvad et al. (2017) indicate that *LA* is more commonly used as a quality requirement than M_{DE}. Considering the moisture level in the tests, the M_{DE} test could be considered better suited to assess aggregates for unbound use, as moisture will be present in the road structure.

One could assume that the amount of material remaining in the original size after testing is a more valuable parameter than the amount of material broken down to 1.6 mm or smaller. However, both Los Angeles and micro-Deval are empirical tests where requirements are set with reference to practical experience (Erichsen et al., 2011). The amount of material broken down from 10–14 mm to smaller than 1.6 mm might not have practical value on its own, but it is related to general experience with the abrasion and fragmentation of unbound aggregates. It is however seen both in the present data and by Erichsen (2015) that a more extensive analysis of the sample gradation after mechanical testing provides valuable knowledge about the degradation properties of the tested material.

4.7. Implications of feed gradation

Including fines in the feed during crushing improves particle shape and reduces specific energy consumption, but can result in a particle size distribution including excess fines, thus requiring an extra screening process to obtain a valuable product gradation. What is gained by a high crushing capacity may be lost due to the need for further processing. The product yield, or the proportion of valuable products vs by-products, has not been part of this study. A simple single-stage crushing plant can be used for various products and the definition of valuable products and by-products depends on the applications. Generally, a high fines content is undesirable because the aggregate material becomes sensitive to moisture and frost.

Moisture content is generally considered an important factor for the stability and compactability of unbound aggregates, as pointed out by e.g. Coronado et al. (2011). However, moisture sensitivity is closely related to the full gradation of the aggregate, and cannot be related to the limited size gradation used in the mechanical tests in the present research. Cook et al. (2017) found that particle shape affects the packing density of unbound aggregates. The full-scale tests conducted in this study shows that both gradation and particle shape can be widely modified by adjusting the production process. A single-stage crushing process including screening equipment can be adjusted to produce aggregates adapted to the gradation suitable for the application.

4.8. Future work

In order to systematically use the knowledge gathered from the full-scale tests, the results should be implemented in models for predicting crusher operation and product quality. The dataset produced in this study could be used to calibrate or validate the model presented by Johansson et al. (2017) regarding capacity, power draw, SEC and particle size prediction.

The data presented here is limited to a single rock type and a single jaw crusher. A natural continuation of this research would be to extend the test programme to include several rock types of varying strength and brittleness. Another possibility is to include other jaw crushers to assess the effect of crusher geometry.

5. Conclusions

The full-scale parameter study allowed for a range of feed material sizes, reduction ratios and crusher operation parameters to be combined. The subsequent quality assessment was conducted using laboratory tests for particle shape and resistance to wear and fragmentation. From the results, the following conclusions can be drawn:

- Particle shape is the quality parameter most affected by variations in the crushing process. The maximal product particle size is highly dependant on the setting of the crusher, so for comparison of particle shape for full gradations, the size range analysed should be related to crusher setting (*CSS*).
- To investigate the effect of changing crusher parameters, analyses of particle shape of individual particle size fractions is necessary in addition to the full size range. The calculation method for flakiness index hides variation of particle shape within a product gradation, increasingly for wider gradations.
- Products in a specific particle size have lower flakiness when produced at a lower *CSS*. However, when flakiness for the full gradation below *CSS* ($FI_{<CSS}$) is analysed, *FI* is independent of *CSS*.
- Reduced crusher speed increases the specific energy consumption of the crushing process by 50–150%, depending on F_{10}. Additionally, the product becomes less well-graded.
- The lower size of the feed material (d and F_{10}) has a significant impact on the product particle shape. *FI* for individual fractions in the sizes 4–50 mm is 2.5–4 times higher when d = 180 mm compared to d = 0 mm
- Reducing the feed rate results in a less well-graded product, and increases the flakiness for particles smaller than the crusher setting. *FI* for individual fractions in the size range 4–50 mm increases by on average 26% when the feed rate is reduced.
- The poor particle shape produced using low feed level and single-graded feed (180/400 mm) shows that inter-particle crushing is a prerequisite for cubical shape.
- Mechanical strength should not be assumed constant for all products produced from a specific rock deposit. Also, mechanical properties are highly affected by sample preparation; laboratory crushed samples are not representative of primary crushed aggregates.
- The amount of material remaining in the original test portion size after the LA test (LA_X) is more closely related to the aggregate gradation and particle shape than the standard *LA* value.

The aim for the parameter study was to investigate whether previous research results regarding crusher operation and aggregate quality are valid also for a simple single-stage jaw crusher operation on large-size aggregates. In response to the original hypothesis the results show that crushing efficiency and product quality in terms of particle shape can be controlled. The quality of construction aggregates can be optimised by adjustments to the production process, even for a single-stage crushing process. In order to improve mechanical properties, several crushing steps are needed.

Declaration of Competing Interest

The authors declare that they have no known competing financial interests or personal relationships that could have appeared to influence the work reported in this paper.

Acknowledgements

The study is financed by the Norwegian Public Roads Administration, Metso Minerals and the Research Council of Norway through the industrial innovation project *Use of local materials* (project No. 256541). This article constitutes a part of the main author's PhD degree at Department of Geoscience and Petroleum, NTNU – Norwegian University of Science and Technology.

The field work was conducted at Metso Minerals' test plant in Tampere, Finland during May and June of 2017. The laboratory work took place at the laboratory of Norwegian Public Roads Administration in Trondheim, Norway during 2017 and 2018.

The authors would like to thank workers at Metso Minerals and Norwegian Public Roads Administration for valuable contributions to the field and laboratory work. Thanks also to master student Nils Arne Fjeldstad Luke who took care of a portion of the laboratory testing.

References

Andersson, E., Öjerborn, S., 2014. Estimation of Rock Quality in Road Projects from Pre-Study to Aggregate (Master thesis). Chalmers University of Technology.

Benediktsson, S., 2015. Effects of Particle Shape on Mechanical Properties of Aggregates (Master thesis). Norwegian University of Science and Technology.

Bengtsson, M., 2009. Quality-Driven Production of Aggregates in Crushing Plants (Phd thesis). Chalmers University of Technology.

Bengtsson, M., Evertsson, C.M., 2006. An empirical model for predicting flakiness in cone crushing. Int. J. Miner. Process. 79 (1), 49–60. https://doi.org/10.1016/j.minpro.2005.12.002.

Bouquety, M., Descantes, Y., Barcelo, L., de Larrard, F., Clavaud, B., 2007. Experimental study of crushed aggregate shape. Constr. Build. Mater. 21 (4), 865–872. https://doi.org/10.1016/j.conbuildmat.2005.12.013.

Brace, W.F., 1961. Dependence of fracture strength of rocks on grain size. In: The 4th U.S. Symposium on Rock Mechanics (USRMS). American Rock Mechanics Association.. https://www.onepetro.org/conference-paper/ARMA-61-099.

Brattli, B., 1992. The influence of geological factors on the mechanical properties of basic igneous rocks used as road surface aggregates. Eng. Geol. 33 (1), 31–44. https://doi.org/10.1016/0013-7952(92)90033-U.

Briggs, C., Evertsson, C., 1998. Shape potential of rock. Miner. Eng. 11 (2), 125–132.

https://doi.org/10.1016/S0892-6875(97)00145-3.
Cook, C.S., Tanyu, B.F., Yavuz, A.B., 2017. Effect of particle shape on durability and performance of unbound aggregate base. J. Mater. Civ. Eng. 29 (2). https://doi.org/10.1061/(ASCE)MT.1943-5533.0001752. 04016 221.
Coronado, O., Caicedo, B., Taibi, S., Correia, A.G., Fleureau, J.M., 2011. A macro geomechanical approach to rank non-standard unbound granular materials for pavements. Eng. Geol. 119 (1–2), 64–73. https://doi.org/10.1016/j.enggeo.2011.02.003.
Eloranta, J., 1995. Influence of Crushing Process Variables on the Product Quality of Crushed Rock (Ph.D. thesis). Tampere University of Technology, Tampere, Finland.
EN 1097-1, 2011. Tests for mechanical and physical properties of aggregates - Part 1: Determination of the resistance to wear (micro-Deval) EN 1097-1:2011. European Committee for Standardization, Brussels, Belgium.
EN 1097-2, 2010. Tests for mechanical and physical properties of aggregates - Part 2: Methods for the determination of resistance to fragmentation EN 1097-2:2010. European Committee for Standardization, Brussels, Belgium.
EN 13242, 2007. Aggregates for Unbound and Hydraulically Bound Materials for Use in Civil Engineering Work and Road Construction EN 13242:2002 + A1:2007. European Committee for Standardization, Brussels, Belgium.
EN 13285, 2018. Unbound mixtures - Specifications EN 13285:2018. European Committee for Standardization, Brussels, Belgium.
EN 933-1, 2012. Tests for geometrical properties of aggregates - Part 1: Determination of particle size distribution - Sieving method EN 933-1:2012. European Committee for Standardization, Brussels, Belgium.
EN 933-3, 2012. Tests for Geometrical Properties of Aggregates - Part 3: Determination of Particle Shape - Flakiness Index EN 933-3:2012. European Committee for Standardization, Brussels, Belgium.
Erichsen, E., 2015. Plotting aggregate degradation results from the Los Angeles test on a triangular diagram: proposal of a new quality ranking for aggregates. Bull. Eng. Geol. Environ. 74 (2), 667–671. https://doi.org/10.1007/s10064-014-0655-z.
Erichsen, E., Ulvik, A., Sævik, K., 2011. Mechanical degradation of aggregate by the Los Angeles-, the Micro-Deval- and the nordic test methods. Rock Mech. Rock Eng. 44 (3), 333–337. https://doi.org/10.1007/s00603-011-0140-y.
Erichsen, E., Ulvik, A., Wolden, K., Neeb, P.R., 2008. Aggregates in Norway - Properties defining the quality of sand, gravel and hard rock for use as aggregate for building purposes. In: Slagstad, T. (Ed.), Geology for Society, Geological Survey of Norway Special Publication, 11. Geological Survey of Norway, Trondheim, Norway, pp. 37–46. http://www.ngu.no/upload/Publikasjoner/Specialpublication/SP11_LO.pdf.
Fladvad, M., Aurstad, J., Wigum, B.J., 2017. Comparison of practice for aggregate use in road construction - results from an international survey. In: Loizos, A., Al-Qadi, I., Scarpas, T. (Eds.), Bearing Capacity of Roads, Railways and Airfields: Proceedings of the 10th International Conference on the Bearing Capacity of Roads, Railways and Airfields (BCRRA 2017), June 28–30, 2017, Athens, Greece. CRC Press, Athens, Greece. pp. 563–570, ISBN 9781138295957.
Guimaraes, M., Valdes, J., Palomino, A., Santamarina, J., 2007. Aggregate production: fines generation during rock crushing. Int. J. Miner. Process. 81 (4), 237–247. https://doi.org/10.1016/j.minpro.2006.08.004.
Johansson, M., Bengtsson, M., Evertsson, M., Hulthén, E., 2017. A fundamental model of an industrial-scale jaw crusher. Miner. Eng. 105, 69–78. https://doi.org/10.1016/j.mineng.2017.01.012.
Lee, E., 2012. Optimization of Compressive Crushing (Ph.D. thesis). Chalmers University of Technology, Göteborg, Sweden.
Miskovsky, K., Taborda Duarte, M., Kou, S., Lindqvist, P.A., 2004. Influence of the mineralogical composition and textural properties on the quality of coarse aggregates. J. Mater. Eng. Perform. 13 (2), 144–150. https://doi.org/10.1361/10599490418334.
Norwegian Public Roads Administration, 2014. Håndbok N200 Vegbygging [Manual N200 Road construction]. Statens vegvesen Vegdirektoratet, Oslo, Norway https://www.vegvesen.no/_attachment/188382/binary/980128?fast_title = Tidligere + utgave%3A + Håndbok + N200 + Vegbygging + 2014 + %2821 + MB%29.pdf.
Norwegian Public Roads Administration, 2016. Håndbok R210 Laboratorieundersøkelser [Manual R210 Laboratory tests]. Statens vegvesen Vegdirektoratet. ISBN 9788272076930. URL https://www.vegvesen.no/_attachment/185231/binary/1276518?fast_title = Håndbok + R210 + Laboratorieundersøkelser + %2811 + MB%29.pdf.
Norwegian Public Roads Administration, 2018. Håndbok N200 Vegbygging [Manual N200 Road construction]. Statens vegvesen Vegdirektoratet, Oslo, Norway ISBN 978-82-7207-723-4. https://www.vegvesen.no/_attachment/2364236/binary/1269980?fast_title = Håndbok + N200 + Vegbygging + %2810 + MB%29.pdf.
NS 3468, 2019. Coarse materials of stone for use in civil engineering works - Specification NS 3468:2019. Standards Norway, Lysaker, Norway.
Räisänen, M., Mertamo, M., 2004. An evaluation of the procedure and results of laboratory crushing in quality assessment of rock aggregate raw materials. Bull. Eng. Geol. Environ. 63 (1), 33–39. https://doi.org/10.1007/s10064-003-0218-1.